Determination of KGa-1b and SHCa-1 $\Delta'^{17}O$ and $\delta^{18}O$ via laser fluorination of lithium fluoride clay pellets

Catherine A. Gagnon[1,2], Riley Havel[1], Jiquan Chen[1,3], Gavin Piccione[1,2], Daniel E. Ibarra[1,2*]

[1]Department of Earth, Environmental, and Planetary Sciences, Brown University, Providence, RI
[2] Institute at Brown for Environment and Society, Brown University, Providence, RI
[3]School of Earth Sciences and Resources, China University of Geosciences (Beijing), Beijing, China
*Corresponding author: daniel_ibarra@brown.edu

Abstract

Rationale

Stable oxygen isotope measurements in silicate clays, such as smectite and kaolinite, provide crucial information for understanding Earth's climate history and environmental changes. Despite a growing interest in the oxygen isotope analysis of silicate clays and clay-rich sediments, there lacks a consensus on the preparation and standardization of clay mineral samples. To improve the accuracy and interlaboratory comparisons of clay isotope measurements, especially those involving laser-fluorination techniques, newly established kaolinite and smectite oxygen isotope standards are much needed.

Methods

We employed conventional nickel bomb fluorination combined with dual-inlet isotope ratio mass spectrometry to establish precise $\delta^{18}O$ and $\Delta'^{17}O$ values for leached clay reference materials KGa-1b and SHCa-1, a kaolinite and a hectorite/smectite, respectively. We further measured leached KGa-1b and SHCa-1 pressed into pellets with a lithium fluoride as a binding agent for the laser fluorination method, allowing us to test the reproducibility between methods and utilize a standard laser chamber drift correction scheme.

Results

The laser fluorination technique yielded highly precise and reproducible $\delta^{18}O$ and $\Delta'^{17}O$ measurements for the KGa-1b and SHCa-1, aligning with bomb values of $\delta^{18}O$. This confirms the method's reliability and comparability to conventional isotope measurement techniques, while also stressing the importance of proper sample preparation and laser chamber drift corrections.

Conclusions

This study demonstrates that laser fluorination is an effective method for accurately measuring the stable oxygen isotope composition of silicate clays or clay-rich sediments when corrected with known silicate clay standards. These methods offer a valuable methodology for future research

and applications, that will significantly improve our understanding of past climate and environmental conditions.

1. Introduction

The stable oxygen isotope ratio ($\delta^{18}O$) of geological materials has been used to understand Earth's system processes for decades[1–3]. Applications include reconstructing climatological changes in temperature[4–6], regional water balance [7–10], global ice [11,12], and the determination of ore formation conditions[13–18]. Silicate clays like smectite or kaolinite are particularly useful for understanding regional weathering processes and water balance since these processes are closely tied to their formation in soils and fluvio-lacustrine settings [19–32]. Further, the oxygen isotope composition of clay weathering products may be combined with modern hydrosphere mass-balance equations to infer past ocean water composition[32]. Despite their demonstrated usefulness in paleoclimate and environmental studies, the methodology for analyzing $\delta^{18}O$ silicate clay has lagged that of more commonly measured sample types, like marine carbonates. For example, measuring the $\delta^{18}O$ value of carbonates has become increasingly more automated through the use of peripheral sample preparation devices since the first measurements were made by hand on a vacuum line in the 1950's and 1960's[33–35].

The first measurements of $\delta^{18}O$ on clay minerals were made in 1963[36] using previously established mineral fluorination techniques[37]. This method involves using either fluorine or an interhalogen fluoride (BrF_5, or ClF_3) to oxidize the clay minerals in nickel rod bombs to O_2 gas, which was then quantitatively converted to CO_2 using heated graphite rods[1,3,19,21,22,27,28,30,38–41]. The carbon dioxide was then purified using liquid nitrogen traps and hot mercury, which removed any residual bromine or fluorine prior to measurement on a mass spectrometer. More recent mass spectrometry methods eliminated the need for conversion of O_2 to CO_2 and instead measured the evolved O_2 gas directly following purification [16,23,25,29,31,42–45].

Since the 1990s laser fluorination has also been used on silicate materials in lieu of nickel reaction tubes (referred throughout as Ni bombs), which allows for smaller sample volume, faster and more complete reactions, and the elimination of hygroscopic contaminant NiF_2 buildup[46]. Laser fluorination is generally reserved for in-situ materials, ore chips, or individual large sample grains, since unconsolidated clay and silt-sized particles often containing highly reactive, hydrous minerals (e.g. phyllosilicates) are subject to dispersion within the laser chamber, partial fluorinations, and vaporization leading to lower sample yield and the depletion of $\delta^{18}O$ values [46–50]. To accurately determine $\delta^{18}O$ of fine-grained materials by laser, homogenized powders are now mixed with a LiF binder and pressed into a pellet prior to loading into the sample holder [23,25,26,42,45,49,51]. The LiF binder physically reduces sample dispersion upon heating, allowing for a more rapid, high-temperature reaction reducing the risk of partial fluorinations and vaporization. Reported $\delta^{18}O$ precision among the various fluorination methods for clay minerals is around 0.2‰ for minerals that do not contain molecular water, such as kaolinite [25,35] and between 0.2‰-0.4‰ for clay minerals with interlayer water, such as smectite [29,35,45]. In most cases, the reported precision for a given clay sample was determined from the repeat analysis of quartz or garnet

standards, not concurrent measurement of clay standards. Only in a few cases were in-house clays, kaolinite or smectite, analyzed alongside quartz or garnet standards for data quality assurance [29,31,45,52].

Recent technological advancements have allowed for the precise measurement of mass-dependent variations of triple oxygen isotopes (^{16}O, ^{17}O, ^{18}O) in silicate materials using the laser methods described above [46,49,53–57]. Small deviations of $\delta'^{18}O$ and $\delta'^{17}O$ from a mass-dependent reference relationship ($\Delta'^{17}O$) [56,58] provide additional context for the interpretation of $\delta^{18}O$ values by constraining isotope effects of kinetic fractionation and other confounding processes that follow different mass law from the typical reference relationship[53,59]. Despite its applicability to terrestrial paleoclimate reconstructions there are currently no studies that have precisely determined the triple oxygen isotope value for pure silicate clay minerals, including widely distributed kaolinite and smectite mineral standards. The closest materials to pure silicate clays analyzed for $\Delta'^{17}O$ include <4μm river sediment collected from major world rivers[32], borehole shales[60], and mixed illite-smectite clay separates from hydrothermally altered mudstones[61].

In the following, we determine the precise $\Delta'^{17}O$ value for two internationally distributed clay mineral standards (KGa-1b and SHCa-1) and one in-house clay (C-6) using laser fluorination of 1:1 LiF-clay pressed pellets. We aim to demonstrate that the determination of $\Delta'^{17}O$ by LiF-clay pellet laser fluorination can achieve similar precision to other commonly measured silicate materials. Secondly, we test the reproducibility of previously reported $\delta^{18}O$ values for KGa-1b [62] and SHCa-1[63] by both laser and bomb fluorination techniques. Lastly, we show that applying a laser chamber drift correction using KGa-1b leads to better precision of unknown clay samples than corrections commonly made using other silicate standards.

2. Isotope notation

Oxygen isotope ratios for $^{17}O/^{16}O$ and $^{18}O/^{16}O$ are reported in standard δ-notation[64] relative to VSMOW-SLAP scale. We also report linearized $\delta^{18}O$ and $\delta^{17}O$ values to account for curvature when making comparisons[65], which are defined as:

$$\delta'^{x}O = 1000\ln(\delta^{x}O/1000 + 1)$$

Where ^{x}O refers to ^{17}O or ^{18}O. Using the δ′-notation, the mass-dependent fractionation between two phases can be written as $1000\ln\alpha_{a\text{-}b} = \delta'^{x}O_a - \delta'^{x}O_b$ and deviations in $\delta'^{17}O$ from a reference slope can be expressed as $\Delta'^{17}O$:

$$\Delta'^{17}O = \delta'^{17}O - \lambda_{RL} \times \delta'^{18}O + \gamma$$

where λ_{RL} is the reference slope and γ is the y-intercept (for this study γ=0). In this work, we adopt a λ_{RL} value of 0.528 consistent with other reported standards within the triple oxygen literature and geological community[43,53,66–69].

3. Methods

3.1 Clay Standards

Kga-1b is a well-crystallized natural kaolinite obtained from the Source Clays Repository of The Clay Mineral Society (CMS). A large aliquot (>100 g) was obtained from C. Page Chamberlain (Stanford University) for this work from bulk material distributed by the Clay Mineral Society. KGa-1b contains 96% kaolinite and trace dickite (3% anatase, 1% crandallite + quartz) [70]. KGa-1b is used to replace the exhausted supply of KGa-1, because of near identical X-ray diffraction (XRD) patterns and only slight mineralogical and chemical differences including higher order crystal phases in KGa-1b [70–73]. While there are no published $\delta^{18}O$ values for KGa-1b, Chapligin et al. (2011) report a value of 21.5 ‰ (VSMOW) for KGa-1 analyzed at the University of Western Ontario. Evidence indicates that, once formed, diagenetic clay minerals may preserve their original isotopic composition, unless subjected to dissolution–reprecipitation reactions [74]. We therefore use the reported KGa-1 $\delta^{18}O$ value for KGa-1b (Table 1) as a point of interlaboratory comparison.

SHCa-1 is a natural hectorite from the Red Mountain Andesite formation in San Bernardino county, CA. As with Kga-1b an aliquot (>100 g) was obtained from Page Chamberlain. This standard was also obtained from the Source Clays Repository. SHCa-1 contains approximately 50% smectite, 43% calcite, 3% dolomite, 3% quartz and 1% other [70]. Reported $\delta^{18}O$ values for SHCa-1 range from 21.2 ‰ to 24.1 ‰ (VSMOW) depending on what pre-treatments were used [63] (Table 1).

C-6 is a Mg-rich pedogenic clay collected from the Uinta alpine zone, which consists of a smectite dominated mixture of kaolinite, illite, and smectite[75] obtained from Jeffrey Munroe. We chose to establish C-6 as an in-house standard because of its low $\delta^{18}O$ value, which falls within the range of natural clay samples from continental settings commonly measured at Brown University[16,61].

In addition to clay standards, known quartz, olivine, garnet, chert, and diatom/diatomite standards [43,54,55,76,77] were also measured during the analysis period (Table 1). The non-pellet standards were used to (1) determine the long-term reference tank $\Delta'^{17}O$ value and (2) monitor the precision and accuracy of the corrected clay $\Delta'^{17}O$ values (details below).

3.2 Sample Preparation

Powdered clay standards were first reacted with a 1M potassium acetate-acetic acid buffer solution (pH=5) to remove any carbonate phases. Samples were then triple rinsed with milli-Q water and re-homogenized via ceramic mortar and pestle. To prevent clay particles from dispersing in the laser chamber during analysis, ~3mg of each sample was then mixed with LiF (1:1 ratio by weight) and pressed into pellets [16,23,25,26,42,45,49,51]. A custom pellet die set with a 2 cm tall chute 0.24 cm in diameter was used to form 0.24 cm pellets, which were loaded into 0.3 cm wide slots in the laser chamber sample holder (Figure 1). A combination of 9-11 pellets and 1-3 non-pellet standards were loaded into sample holder at a time. The loaded sample holder was placed within the laser chamber and dried under vacuum using a molecular turbo pump for 12+ hours, reaching typical backgrounds in the $1x10^{-6}$ millibar range. All samples within the laser chamber were analyzed within an 8–14-hour window the following day.

3.3 Fluorination Methods

The oxygen isotope ratios of the clays pellets were measured via laser fluorination at Brown University Oxygen Isotope Fluorination Lab. At the beginning of each analysis day, the samples were exposed to three 3-5 min preflourinations under vacuum with BrF_5 to liberate impurities from the samples and fluorination line. The O_2 gas was liberated from the samples by reaction with BrF_5 in a 3-5:1 stoichiometric excess while being heated using a 50 W CO_2 infrared laser as described in detail [16,43,61,78]. Briefly, the O_2 gas was passed through a liquid N_2 trap, a NaCl trap, a second liquid N_2 trap, and then sorbed on to a zeolite trap at liquid N_2 temperature. After evacuating remaining non-condensables, the O_2 gas was then passed through a molecular sieve gas chromatography column[43,56,79] to another chilled zeolite using a He carrier gas before being introduced to the sample side bellow of the mass spectrometer after evacuating the He carrier gas.

When analyzing via the conventional Ni bombs roughly 3mg of leached sample powder was added to the nickel bombs. The bombs were then heated to 200 ºC for 2 hours under vacuum afterwards pre-fluorinated 3x for 5 min to remove any surficial contaminants[43,80] BrF_5 at an ~5:1 stoichiometric excess was then added to each reaction vessel and heated to 600 ºC for 16 hours. Once the bomb samples are reacted with BrF_5, the analytical procedure is identical to that of the laser samples. All clay isotopic ratios are reported with respect to Vienna standard mean ocean water (VSMOW) based on corrections described below.

3.4. IRMS Methods

Following laser fluorination and purification, sample O_2 was analyzed on a dual inlet MAT 253+ isotope ratio mass spectrometer. An initial argon background check was performed on each bellow to screen for leaks introduced during the sample reaction and purification steps. Samples that maintained low Ar backgrounds (<3000 mV) were then measured 2-3 times with an integration time of XXs with 10 iterations per analysis and against the same O_2 reference gas. Samples were run at an intensity of 5V on mass 32, corresponding to a pressure of ~25 mbar in the bellows and XX mbar in the source.

3.5 Drift Corrections ($\delta^{18}O$)

There is an observable drift in the measured isotope values of clays analyzed in the laser chamber[25,42]. This drift is likely attributed to the liberation of excess contaminants and interstitial waters throughout the course of the run and/or the partial reaction of clays during subsequent reactions. At least 3 KGa-1b pellets were measured in each chamber in the beginning, middle, and end of the analysis day and used to make daily $\delta^{18}O$ drift corrections. The difference between the measured KGa-1b and the internal bomb determined KGa-1 $\delta^{18}O$ value (21.459 ‰; S1) were plotted against the daily run order, and the resulting linear trend (typical R^2 of 0.25 to 0.91; Table S1) applied to the other clay samples within the laser chamber. Identical corrections were made using an externally determined value for KGa-1 for comparison (Table S2).

Typically, the KGa-1 $\delta^{18}O$ value becomes more positive after applying the correction. The average magnitude of the correction is 0.88 ‰. This correction was only performed on the clay

samples run by laser fluorination. Samples run via conventional Ni bomb fluorination are corrected via a daily offset[43,44].

3.6 Reference Gas Corrections ($\Delta'^{17}O$)

Because there are currently no reported $\Delta'^{17}O$ values for the clay standards, the $\Delta'^{17}O$ corrections for KGa-1b, SHCa-1, and C-6 are made against known non-clay standards measured alongside the clays [16,32,60]. To reserve space for like-material standards and allow for higher sample throughput, we tested using the long-term determined laboratory reference tank $\Delta'^{17}O$ value as a means for making sample chamber corrections and compare the results with the conventional non-clay standard correction method. The assumption is that fractionation in bulk composition ($\delta^{18}O$ values) follows a mass law of ~0.528, as previously assumed in comparable work[69]. Further, this assumption is made to address a practical need for sample throughput because triple oxygen isotope measurements take ~1 to 1.5 hours per sample.

The reference tank calibration to the VSMOW-SLAP scale was achieved by analyzing five known silicate standards by laser over several years (March 2022 to April 2024; Table S3). The calibration to the VSMOW-SLAP scale also involves the determination of the compression scale factor, which is unique for each mass-spectrometer and reflects its deviation from perfect linearity of slope 1.00 across a wide range of δ values[81]. Repeat analysis of silicate standards over time has allowed for the determination of the compression factor of the Brown University MAT 253+ and the transformation of its measurements to the VSMOW-SLAP scale. The results with an r^2 value of 0.9993 for $\delta'^{18}O$ and 0.9993 for $\delta'^{17}O$, respectively, with slopes of 1.0019 and 1.0017, respectively, cover a range of 60‰ in $\delta^{18}O$ and via the intercept values provide the calibrated $\delta'^{18}O$ and $\delta'^{17}O$ values and thus the $\Delta''^{17}O$ of the Brown University MAT 253+ reference gas (Figure 2; $\delta'^{18}O$ = -10.0296; $\delta'^{17}O$ = -5.2560; $\Delta'^{17}O$ = +0.00396 ‰).

4. Results

In the following, we report and compare the values obtained using multiple correction schemes. For clarity, we define them here. Correcting via "daily offset" pertains to samples that have been corrected to the average daily offset of the non-clay silicate standards run in that day's laser chamber or bomb set (Table S5). This is the traditional method of standard correction. Correcting via "the known reference tank value" corresponds to isotope values that were corrected using the previously established known value for the reference tank (see above section).

4.1. KGa-1b

The laser KGa-1b $\delta^{18}O$ values corrected via daily offset from non-clay standards have a value of 19.787‰ (±1.000 (1σ); ±0.158 (1SE); n=40) (Table 2; Table S1), while the conventional Ni bomb value corrected via daily offset is 21.459 (±0.771 (1σ); ±0.257 (1SE); n=9) (Table S4). In addition to the laser-produced clay $\delta^{18}O$ values being generally lower than bomb-produced clay $\delta^{18}O$ values, laser-produced clay $\delta^{18}O$ values experienced on average a 0.996‰ magnitude drift between the first and last sample analyzed each day.

The drift-corrected laser fluorination $\delta^{18}O$ value for KGa-1b is 21.478‰ (±0.267 (1σ); ±0.042 (1SE); n=40) (Figure 1; Table S1) when made using the reference tank value and 21.427‰ (±0.948 (1σ); ±0.03 (1SE); n=40) when corrected via non-clay chamber standards. The laser fluorination-based $\Delta'^{17}O$ value for KGa-1b is -0.074 (±0.014 (1σ); ±0.002 (1SE); n=40) when the correction is made using the known reference tank value (Figure 3; Table S1). The laser fluorination based $\Delta'^{17}O$ value is nearly identical to the mean conventional Ni bomb $\Delta'^{17}O$ value, which is -0.073 (±0.014 (1σ); ±0.005 (1SE); n=9) and corrected by non-clay bomb standards (Table S4). When corrected using the non-clay chamber standards, the drift corrected laser fluorination-based $\Delta'^{17}O$ value for KGa-1b is -0.067 (±0.017 (1σ); ±0.003 (1SE); n=40) (Table S1).

4.2. SHCa-1

The mean drift-corrected laser fluorination $\delta^{18}O$ value for SHCa-1 is 21.769‰ (±0.753 (1σ); ±0.227 (1SE); n=11) when corrected against the reference tank value (Figure 3) and 21.784‰ (±1.102 (1σ); ±0.348 (1SE); n=11) when corrected by non-clay chamber standards (Table S1). The conventional Ni bomb value corrected via daily standard offsets is 22.042‰ (±0.830 (1σ); ±0.338 (1SE); n=5) (Table 2; Table S4). The mean laser fluorination-based $\Delta'^{17}O$ value for SHCa-1 is -0.1162‰ (±0.0073 (1σ); ±0.0023 (1SE); n=11) when corrected daily against non-clay chamber standards and -0.1222‰ (±0.0078 (1σ); ±0.0023 (1SE); n=11) when corrected against the long-term reference tank value (Table S1). The mean conventional Ni bomb $\Delta'^{17}O$ value is -0.1083‰ (±0.016 (1σ); ±0.007 (1SE); n=5) when corrected via chamber standards, and -0.1005‰ (±0.014 (1σ); ±0.006 (1SE); n=5) when corrected using the reference tank value (Table S4). The bomb-determined $\Delta'^{17}O$ and $\delta^{18}O$ values for SHCa-1 are higher than the laser-determined values.

4.3. C-6

The mean drift-corrected laser fluorination $\delta^{18}O$ value for the unknown C-6 is 13.577‰ (±1.141 (1σ); ±0.277 (1SE); n=17) when corrected against the reference tank value (Figure 3; Table 2) and 13.261‰ (±1.360 (1σ); ±0.330 (1SE); n=17) when corrected using non-clay chamber standards (Table S1). The mean laser fluorination-based $\Delta'^{17}O$ value for C-6 is -0.1056 (±0.0131 (1σ); ±0.0032 (1SE); n=17) when corrected using the tank value and -0.0993 (±0.0155 (1σ); ±0.0038 (1SE); n=17) when corrected using non-clay chamber standards. No C-6 samples were analyzed via bomb.

Discussion

5.1. New standards for clay-rich geologic materials

KGa-1b, SHCa-1, or C-6 are ideal standards for assessing the quality of $\Delta'^{17}O$ and $\delta^{18}O$ data generated from clay-rich geological materials, because of similar mineralogy, grain size, and consequently reactivity. Further, when plotted in $\Delta'^{17}O$-$\delta^{18}O$ space, the isotopic composition of KGa-1b, SHCa-1, and C-6 fall within the same field as clay-rich shales[60] , mixed illite and smectite

clays from hydrothermally altered mudstones[61], and mixed clays from rivers around the world [32] (Figure 4). This is particularly useful considering most clay materials plotted in a region ($\delta'^{18}O$=3.24 to 19.96 ‰ and $\Delta'^{17}O$= -0.17 to -0.06 ‰) under-represented by existing inter-laboratory silicate standards (Figure 4). As such, we propose that KGa-1b and SHCa-1, both widely distributed clay mineral materials, can be used by other groups and laboratories as either primary or secondary standards to allow for more direct interlaboratory comparisons between clay-rich sediments or clay separates. For example, if leaching protocols can be standardized for oxygen isotope analyses (beyond the scope of this work), like recent efforts by Kanik et al. (2022) for δD measurements, these two clay mineral standards appear suitable for use to ensure cross-laboratory intercalibration of $\Delta'^{17}O$-$\delta^{18}O$.

The drift-corrected laser fluorination $\delta^{18}O$ value for SHCa-1 is within 0.1‰ accuracy of values reported by Fagan and Longstaffe (1996) for sodium acetate treated SHCa-1 samples analyzed by bomb. Our bomb-produced clay $\delta^{18}O$ value is slightly lower, but accurate within 0.16 ‰ of the sodium acetate treated SHCa-1 samples[63]. The incomplete fluorination of SHCa-1 with BrF_5 within the nickel bombs may account for the unexpected low bomb-produced clay $\delta^{18}O$ values. In this case, slow and low-temperature reactions can lead to the vaporization of SiO_2, which preferentially preserves Si–^{18}O bonds and results in lower O_2 yields and $\delta^{18}O$ values[49]. High temperature reactions involving methanation prior to fluorination (Ellis and Passey, 2023) are shown to generate more complete reactions in organic materials and could perhaps also curb these effects in analogous reactions. Alternatively, laser-produced clay $\delta^{18}O$ values are higher than bomb-produced clay $\delta^{18}O$ values due to the repeat exposure of the sample to BrF_5 and resulting passive fluorination over the course of the analysis day. This phenomenon, only observed in very fine-grained hydrous phases, preferentially liberates ^{16}O, resulting in higher residual clay $\delta^{18}O$ values[49]. The effects of passive fluorination are likely higher for SHCa-1 compared to KGa-1b, considering hectorite has a higher capacity for structural waters than kaolinite via a higher specific surface area and thus may react more readily. Drift corrections based on KGa-1b may therefore underestimate these effects in smectites.

5.2. Proposed method for the laser determination of $\Delta'^{17}O$ and $\delta^{18}O$ in clay materials

In this work, clay samples were standardized to the VSMOW-SLAP scale by adjusting them based on known 2-3 silicate standards analyzed in the same laser chamber on the same day. Additionally, internal clay standards were analyzed in the same chamber to account for any drift related to the clay materials. The combination of clay and non-clay standards restricts the number of unknown samples that can be feasibly run in each day. We instead propose that our newly determined bomb-produced clay $\delta^{18}O$ value for KGa-1b (21.459‰ ±0.771 (1σ)) and laser determined $\Delta'^{17}O$ value for Kga-1b (-0.0735‰ ±0.0144 (1σ)) be used as a primary standard for the analysis of $\delta^{18}O$ and $\Delta'^{17}O$ of clay materials, which eliminates the need for additional non-clay standards.

Practical considerations for standardization of clay materials include necessary pretreatments, the number and type of samples and standards to be analyzed per day (limited by the 60-to-90-minute measurement on the IRMS), and whether the $\Delta'^{17}O$ value of a given lab's

reference tank is precisely known. Aliquots of KGa-1b obtained from CMS should be leached prior to isotope analysis, to be consistent with established pretreatments necessary for clay mineral separation. When analyzing via laser fluorination, no less than 3 KGa-1b pellets should be analyzed across the beginning, middle, and end of day. These standards should be used to apply a daily drift correction normalized to our accepted bomb value for KGa-1b. The laser chamber may then contain up to 9 additional samples or standards, which would typically equate to a 12–14-hour analysis period. If the $\Delta'^{17}O$ of the dual inlet reference tank is precisely known, up to 9 remaining sample slots may be filled with unknowns. Otherwise, we recommend analyzing an additional non-clay silicate standard in addition to KGa-1b when correcting $\Delta'^{17}O$ values.

6. Conclusion

Advancements in the stable oxygen isotope analysis of silicate clays, particularly kaolinite and smectite, have provided significant insights into paleoclimate and environmental studies. However, a consensus is lacking on the proper preparation and standardization of clay minerals, which are much more susceptible to isotopic drift from incomplete reactions and contamination than standard silicate materials. By employing a combination of LiF-clay pellet preparation and laser fluorination methods, this study demonstrates the capability to achieve high precision in $\delta^{18}O$ and $\Delta'^{17}O$ values for kaolinite and smectite, comparable to those of other silicate materials. The findings affirm that KGa-1b and SHCa-1 can serve as reliable standards for oxygen isotope analysis in clay-rich materials, promoting consistent interlaboratory calibration. Furthermore, the study underscores the importance of standardizing leaching protocols and correcting for procedural drifts to enhance the accuracy of clay isotope data.

Acknowledgements and Funding

We thank Joe Orchardo and Steve Clemens for support in laboratory analyses; C. Page Chamberlain for providing the clay mineral standards and methodological discussions; Cameron Meyers and Greg Hirth for help with pellet press methodology. We thank Fred Longstaffe for sharing internal standard values. Gagnon was partially supported by NSF AGS 2102901 to Ibarra; Piccione was partially supported by NSF EAR 2303484 to Ibarra; and Havel was supported by NSF GRFP (Grant no. 2040433).

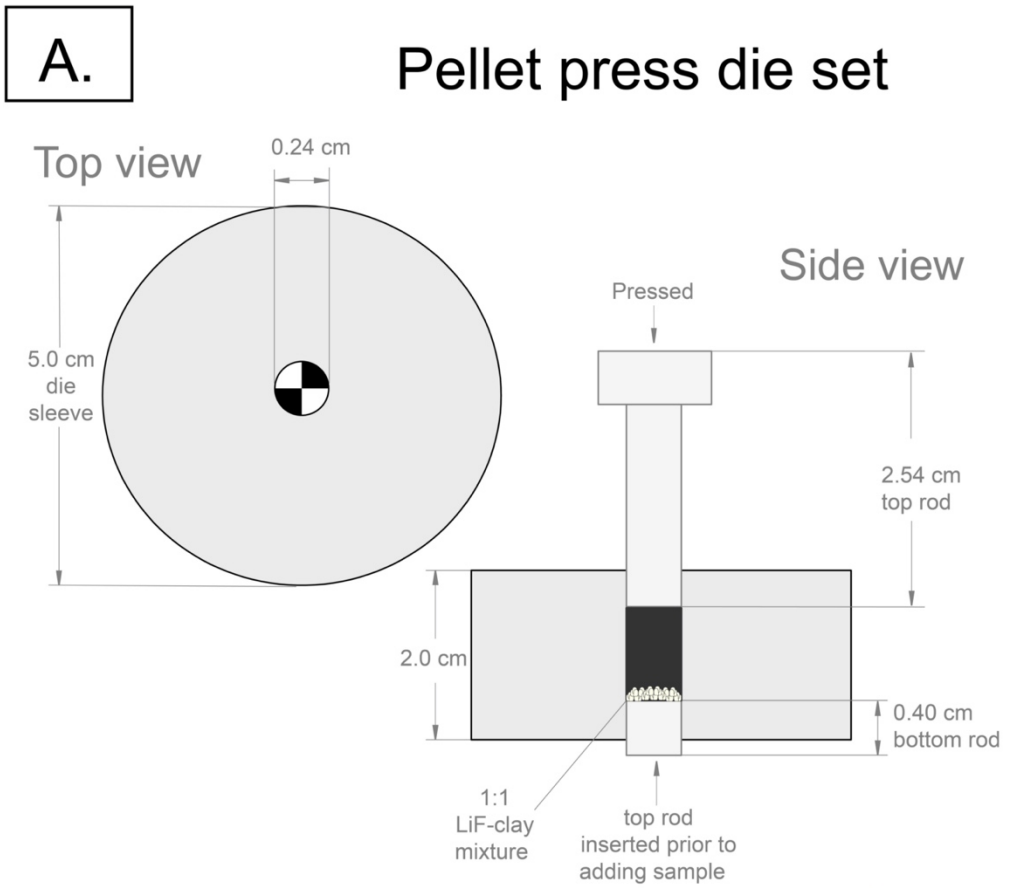

Figure 1. (A) Die set used to form clay pellets and (B) laser chamber sample holder containing 11 prepared pellets and 1 non-pellet standard typical of one daily analysis period.

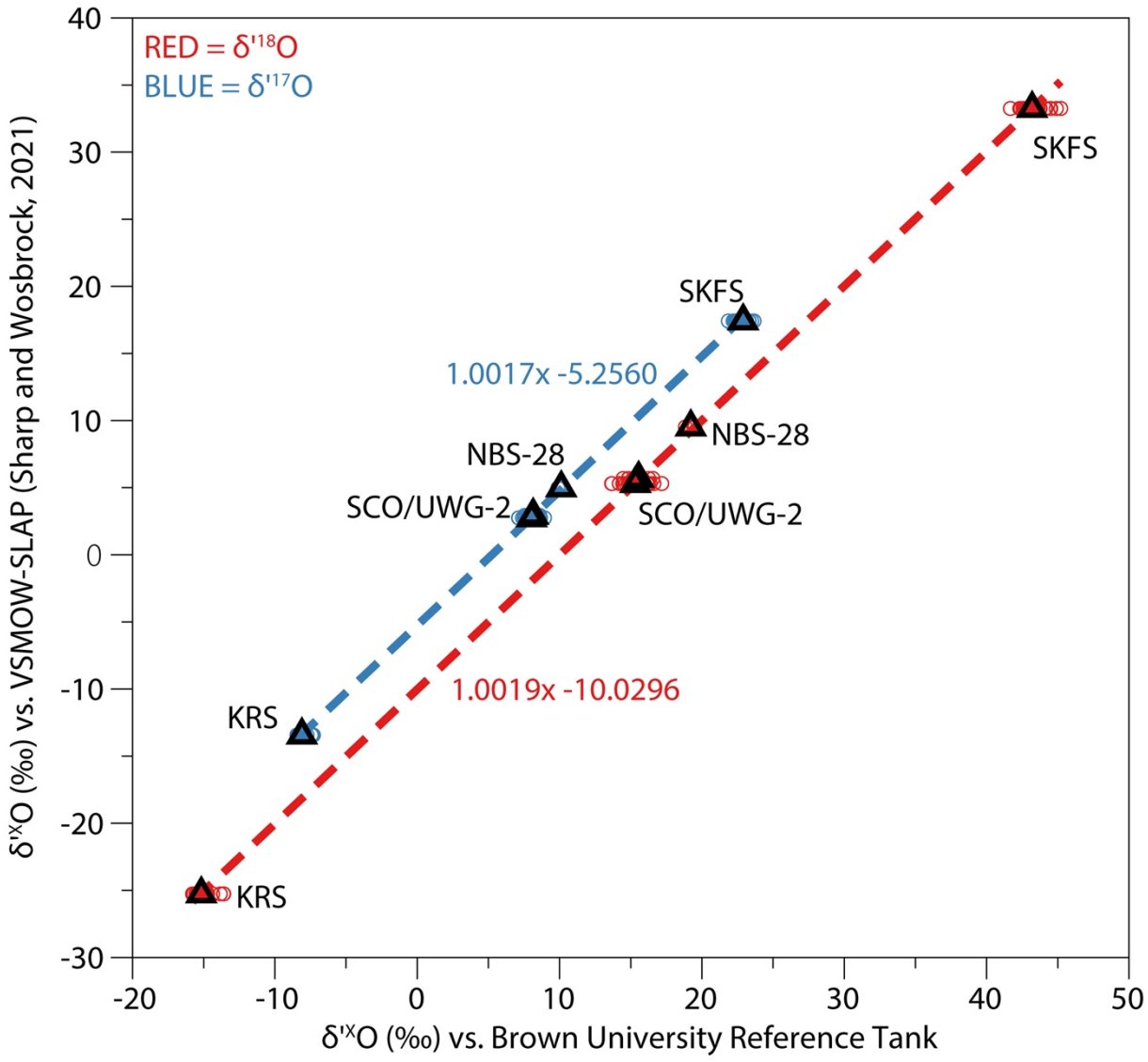

Figure 2. Measured isotope values vs the Brown University reference tank against the known standard values in VSMOW-SLAP for both $\delta'^{18}O$ (red) and $\delta'^{17}O$ (blue) (Table S3). Known values are taken from the multi-laboratory average given in Sharp and Wostbrock (2021) (their Table 1).

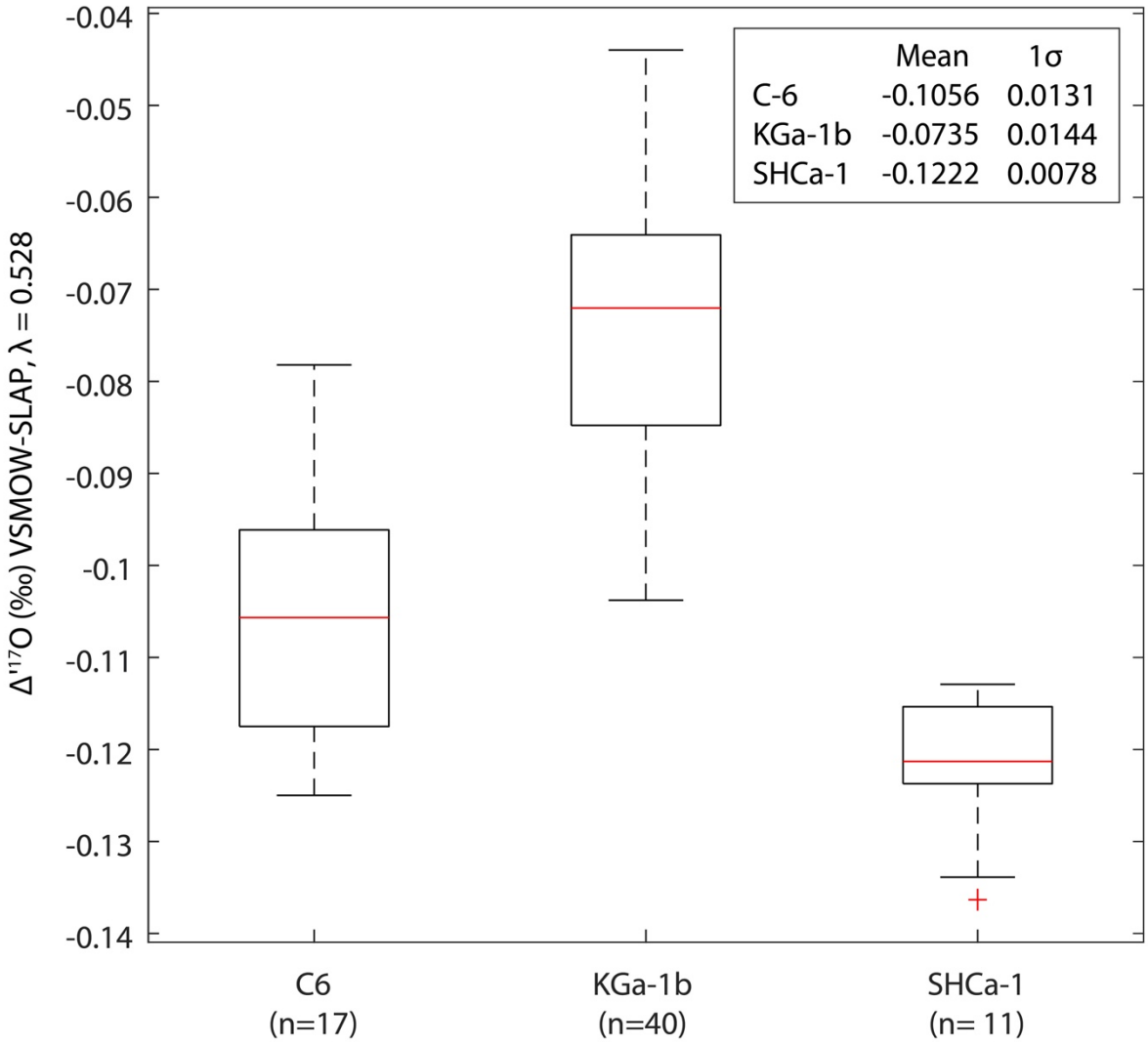

Figure 3. Reference tank corrected $\Delta'^{17}O$ values measured by laser for C-6, KGa-1b, and SHCa-1 shown using box and whisker plots.

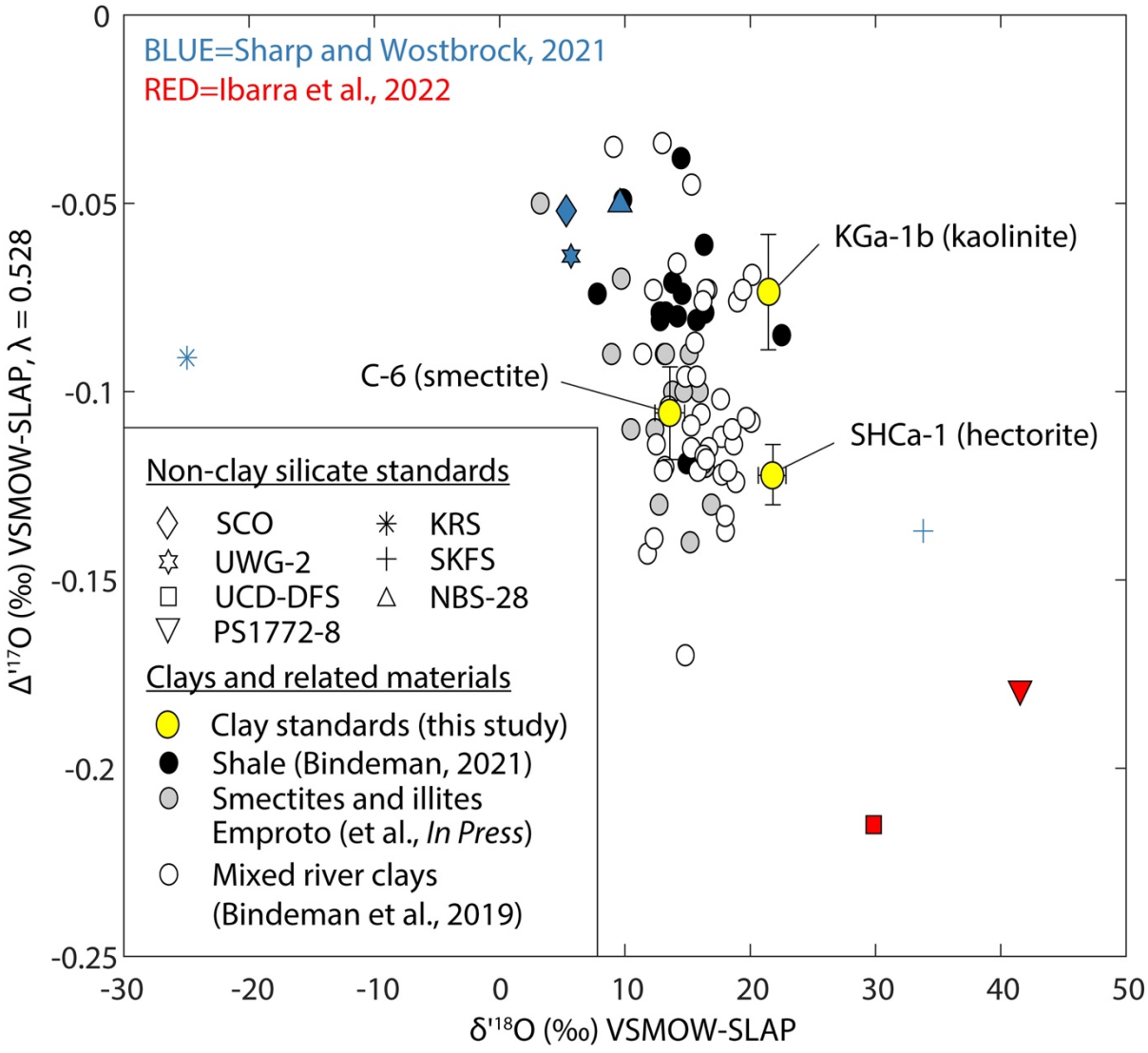

Figure 4. Comparison of newly established clay mineral standard values (this study, yellow) to well-established non-clay silicate standard values (blue and red) and clay-rich geological samples (black, gray, and white) plotted within the $\Delta'^{17}O$-$\delta^{18}O$ reference frame.

References

1. O'Neil JR, Kharaka YK. Hydrogen and oxygen isotope exchange reactions between clay minerals and water. *Geochim Cosmochim Acta*. 1976;40(2):241-246.
2. Urey HC. The thermodynamic properties of isotopic substances. *Journal of the Chemical Society (Resumed)*. 1947;(0):562-581. doi:10.1039/JR9470000562
3. Savin SM, Epstein S. The oyxgen and hydrogen isotope geochemistry of ocean sediments and shales. *Geochim Cosmochim Acta*. 1970;34(1):43-63.
4. Zachos J, Pagani M, Sloan L, Thomas E, Billups K. Trends, rhythms, and aberrations in global climate 65 Ma to present. *Science (1979)*. 2001;292(5517):686-693.
5. Erez J, Luz B. Experimental paleotemperature equation for planktonic foraminifera. *Geochim Cosmochim Acta*. 1983;47(6):1025-1031.
6. Prentice ML, Matthews RK. Cenozoic ice-volume history: development of a composite oxygen isotope record. *Geology*. 1988;16(11):963-966.
7. Gat JR. Oxygen and hydrogen isotopes in the hydrologic cycle. *Annu Rev Earth Planet Sci*. 1996;24(1):225-262.
8. Dee S, Bailey A, Conroy JL, et al. Water isotopes, climate variability, and the hydrological cycle: recent advances and new frontiers. *Environmental Research: Climate*. 2023;2(2):022002.
9. Dansgaard W. Stable isotopes in precipitation. *Tellus*. 1964;16(4):436-468. doi:https://doi.org/10.1111/j.2153-3490.1964.tb00181.x
10. Konecky BL, McKay NP, Churakova (Sidorova) O V, et al. The Iso2k database: a global compilation of paleo-δ18O and δ2H records to aid understanding of Common Era climate. *Earth Syst Sci Data*. 2020;12(3):2261-2288. doi:10.5194/essd-12-2261-2020
11. Raymo ME, Lisiecki LE, Nisancioglu KH. Plio-Pleistocene ice volume, Antarctic climate, and the global δ18O record. *Science (1979)*. 2006;313(5786):492-495.
12. Shakun JD, Lea DW, Lisiecki LE, Raymo ME. An 800-kyr record of global surface ocean δ18O and implications for ice volume-temperature coupling. *Earth Planet Sci Lett*. 2015;426:58-68. doi:https://doi.org/10.1016/j.epsl.2015.05.042
13. Pacey A, Wilkinson JJ, Boyce AJ, Millar IL. Magmatic Fluids Implicated in the Formation of Propylitic Alteration: Oxygen, Hydrogen, and Strontium Isotope Constraints from the Northparkes Porphyry Cu-Au District, New South Wales, Australia. *Economic Geology*. 2020;115(4):729-748. doi:10.5382/econgeo.4732
14. Huston DL, Trumbull RB, Beaudoin G, Ireland T. Light stable isotopes (H, B, C, O and S) in ore studies—methods, theory, applications and uncertainties. In: *Isotopes in Economic Geology, Metallogenesis and Exploration*. Springer; 2023:209-244.
15. Bindeman HN, Valley JW. Oxygen isotope study of the Long Valley magma system, California: Isotope thermometry and convection in large silicic magma bodies. *Contributions to Mineralogy and Petrology*. 2002;144(2):185-205. doi:10.1007/s00410-002-0371-8
16. Gagnon CA, Butler KL, Robertson K, et al. *Economic Geology VOLCANO-SEDIMENTARY LITHIUM OCCURRENCES IN BARSTOW, CA AND THEIR RELATED FORMATION MECHANISMS DETERMINED BY STABLE ISOTOPE ANALYSES OF CARBONATES AND CLAYS.*
17. Wagner T, Mlynarczyk MSJ, Williams-Jones AE, Boyce AJ. Stable Isotope Constraints on Ore Formation at the San Rafael Tin-Copper Deposit, Southeast Peru. *Economic Geology*. 2009;104(2):223-248. doi:10.2113/gsecongeo.104.2.223

18. Wilkinson JJ. Fluid inclusions in hydrothermal ore deposits. *Lithos*. 2001;55(1):229-272. doi:https://doi.org/10.1016/S0024-4937(00)00047-5
19. Gilg HA, Hall AM, Ebert K, Fallick AE. Cool kaolins in Finland. *Palaeogeogr Palaeoclimatol Palaeoecol*. 2013;392:454-462.
20. Gilg HA. D–H evidence for the timing of kaolinization in Northeast Bavaria, Germany. *Chem Geol*. 2000;170(1-4):5-18.
21. Mora G, Pratt LM. Isotopic evidence for cooler and drier conditions in the tropical Andes during the last glacial stage. *Geology*. 2001;29(6):519-522.
22. Rosenau NA, Tabor NJ. Oxygen and hydrogen isotope compositions of paleosol phyllosilicates: differential burial histories and determination of Middle–Late Pennsylvanian low-latitude terrestrial paleotemperatures. *Palaeogeogr Palaeoclimatol Palaeoecol*. 2013;392:382-397.
23. Mix HT, Chamberlain CP. Stable isotope records of hydrologic change and paleotemperature from smectite in Cenozoic western North America. *Geochim Cosmochim Acta*. 2014;141:532-546.
24. Hall AM, Gilg HA, Fallick AE, Merritt JW. Kaolins in gravels and saprolites in north-east Scotland: Evidence from stable H and O isotopes for Palaeocene–Miocene deep weathering. *Palaeogeogr Palaeoclimatol Palaeoecol*. 2015;424:6-16.
25. Mix HT, Ibarra DE, Mulch A, Graham SA, Chamberlain CP. A hot and high Eocene Sierra Nevada. *Bulletin*. 2016;128(3-4):531-542.
26. Gao Y, Gao Y, Ibarra DE, et al. Clay mineralogical evidence for mid-latitude terrestrial climate change from the latest Cretaceous through the earliest Paleogene in the Songliao Basin, NE China. *Cretac Res*. 2021;124:104827.
27. Stern LA, Chamberlain CP, Reynolds RC, Johnson GD. Oxygen isotope evidence of climate change from pedogenic clay minerals in the Himalayan molasse. *Geochim Cosmochim Acta*. 1997;61(4):731-744.
28. Vitali F, Longstaffe FJ, McCarthy PJ, Plint AG, Caldwell WGE. Stable isotopic investigation of clay minerals and pedogenesis in an interfluve paleosol from the Cenomanian Dunvegan Formation, NE British Columbia, Canada. *Chem Geol*. 2002;192(3-4):269-287.
29. Sjostrom DJ, Hren MT, Horton TW, Waldbauer JR, Chamberlain CP. Stable isotopic evidence for a pre–late Miocene elevation gradient in the Great Plains–Rocky Mountain region, USA. Published online 2006.
30. Feng W, Yapp CJ. 18O/16O and D/H ratios of pedogenic kaolinite in a North American Cenomanian laterite: Paleoclimatic implications. *Geochim Cosmochim Acta*. 2009;73(20):6249-6263.
31. Muttik N, Kirsimäe K, Vennemann TW. Stable isotope composition of smectite in suevites at the Ries crater, Germany: Implications for hydrous alteration of impactites. *Earth Planet Sci Lett*. 2010;299(1-2):190-195.
32. Bindeman IN, Bayon G, Palandri J. Triple oxygen isotope investigation of fine-grained sediments from major world's rivers: Insights into weathering processes and global fluxes into the hydrosphere. *Earth Planet Sci Lett*. 2019;528:115851.
33. Keith ML, Weber JN. Carbon and oxygen isotopic composition of selected limestones and fossils. *Geochim Cosmochim Acta*. 1964;28(10-11):1787-1816.
34. Degens ET, Epstein S. Oxygen and carbon isotope ratios in coexisting calcites and dolomites from recent and ancient sediments. *Geochim Cosmochim Acta*. 1964;28(1):23-44.

35. Epstein S, Buchsbaum R, Lowenstam H, Urey HC. Carbonate-water isotopic temperature scale. *Geol Soc Am Bull*. 1951;62(4):417-426.
36. Clayton RN, Mayeda TK. The use of bromine pentafluoride in the extraction of oxygen from oxides and silicates for isotopic analysis. *Geochim Cosmochim Acta*. 1963;27(1):43-52.
37. TAYLOR JR. HP, EPSTEIN S. Relationship Between O18/O16 Ratios in Coexisting Minerals of Igneous and Metamorphic Rocks: Part 1: Principles and Experimental Results. *GSA Bulletin*. 1962;73(4):461-480. doi:10.1130/0016-7606(1962)73[461:RBORIC]2.0.CO;2
38. Chamberlain CP, Poage MA, Craw D, Reynolds RC. Topographic development of the Southern Alps recorded by the isotopic composition of authigenic clay minerals, South Island, New Zealand. *Chem Geol*. 1999;155(3-4):279-294.
39. Girard JP, Freyssinet P, Chazot G. Unraveling climatic changes from intraprofile variation in oxygen and hydrogen isotopic composition of goethite and kaolinite in laterites: an integrated study from Yaou, French Guiana. *Geochim Cosmochim Acta*. 2000;64(3):409-426.
40. Tabor NJ, Montanez IP. Shifts in late Paleozoic atmospheric circulation over western equatorial Pangea: Insights from pedogenic mineral δ18O compositions. *Geology*. 2002;30(12):1127-1130.
41. Tabor NJ, Montañez IP. Oxygen and hydrogen isotope compositions of Permian pedogenic phyllosilicates: Development of modern surface domain arrays and implications for paleotemperature reconstructions. *Palaeogeogr Palaeoclimatol Palaeoecol*. 2005;223(1-2):127-146.
42. Pope EC, Bird DK, Arnórsson S. Evolution of low-18O Icelandic crust. *Earth Planet Sci Lett*. 2013;374:47-59.
43. Ibarra DE, Yanchilina AG, Lloyd MK, et al. Triple oxygen isotope systematics of diagenetic recrystallization of diatom opal-A to opal-CT to microquartz in deep sea sediments. *Geochim Cosmochim Acta*. 2022;320:304-323.
44. Ibarra DE, Dai J, Gao Y, et al. High-elevation Tibetan Plateau before India–Eurasia collision recorded by triple oxygen isotopes. *Nat Geosci*. 2023;16(9):810-815.
45. Kukla T, Ibarra DE, Rugenstein JKC, et al. High-Resolution Stable Isotope Paleotopography of the John Day Region, Oregon, United States. *Front Earth Sci (Lausanne)*. 2021;9:635181.
46. Sharp ZD. A laser-based microanalytical method for the in situ determination of oxygen isotope ratios of silicates and oxides. *Geochim Cosmochim Acta*. 1990;54(5):1353-1357. doi:https://doi.org/10.1016/0016-7037(90)90160-M
47. Rowe MW, Clayton RN, Mayeda TK. Oxygen isotopes in separated components of CI and CM meteorites. *Geochim Cosmochim Acta*. 1994;58(23):5341-5347.
48. Fouillac AM, Girard JP. Laser oxygen isotope analysis of silicate/oxide grain separates: Evidence for a grain size effect? *Chem Geol*. 1996;130(1-2):31-54.
49. Kirschner DL, Sharp ZD. Oxygen isotope analyses of fine-grained minerals and rocks using the laser-extraction technique. *Chem Geol*. 1997;137(1-2):109-115.
50. Ghoshmaulik S, Bhattacharya SK, Roy P, Sarkar A. A simple cryogenic method for efficient analysis of triple oxygen isotopes in silicates. *Rapid Communications in Mass Spectrometry*. 2020;34(18):e8833.
51. Kukla T, Rugenstein JKC, Ibarra DE, Winnick MJ, Strömberg CAE, Chamberlain CP. Drier winters drove Cenozoic open habitat expansion in North America. *AGU Advances*. 2022;3(2):e2021AV000566.

52. Mix HT, Chamberlain CP. Stable isotope records of hydrologic change and paleotemperature from smectite in Cenozoic western North America. *Geochim Cosmochim Acta*. 2014;141:532-546.
53. Sharp ZD, Wostbrock JAG, Pack A. Mass-dependent triple oxygen isotope variations in terrestrial materials. *Geochem Perspect Lett*. 2018;7:27-31.
54. Sharp ZD, Wostbrock JAG. Standardization for the Triple Oxygen Isotope System: Waters, Silicates, Carbonates, Air, and Sulfates. *Rev Mineral Geochem*. 2021;86(1):179-196. doi:10.2138/rmg.2021.86.05
55. Wostbrock JAG, Cano EJ, Sharp ZD. An internally consistent triple oxygen isotope calibration of standards for silicates, carbonates and air relative to VSMOW2 and SLAP2. *Chem Geol*. 2020;533:119432. doi:https://doi.org/10.1016/j.chemgeo.2019.119432
56. Pack A, Herwartz D. The triple oxygen isotope composition of the Earth mantle and understanding ΔO17 variations in terrestrial rocks and minerals. *Earth Planet Sci Lett*. 2014;390:138-145.
57. Hofmann MEG, Pack A. Technique for high-precision analysis of triple oxygen isotope ratios in carbon dioxide. *Anal Chem*. 2010;82(11):4357-4361.
58. Luz B, Barkan E. Variations of 17O/16O and 18O/16O in meteoric waters. *Geochim Cosmochim Acta*. 2010;74(22):6276-6286.
59. Aron PG, Levin NE, Beverly EJ, et al. Triple oxygen isotopes in the water cycle. *Chem Geol*. 2021;565:120026.
60. Bindeman IN. Triple oxygen isotopes in evolving continental crust, granites, and clastic sediments. *Rev Mineral Geochem*. 2021;86(1):241-290.
61. Emproto C, Benson TR, Gagnon CA, Baek W, Ibarra DE, Simon AC. Clay Chemistry of the Thacker Pass Deposit, Nevada: Implications for the Formation of High-grade Volcano-sedimentary Lithium Resources. *Economic Geology*.
62. Chapligin B, Leng MJ, Webb E, et al. Inter-laboratory comparison of oxygen isotope compositions from biogenic silica. *Geochim Cosmochim Acta*. 2011;75(22):7242-7256.
63. Fagan R, Longstaffe F. The effects of laboratory pretreatments on the hydrogen-and oxygen-isotope compositions of clay minerals. In: *Clays in and for the Environment. 33rd Annual Meeting of the Clay Minerals Society, Program and Abstracts* . ; 1996:55.
64. McKinney CR, McCrea JM, Epstein S, Allen HA, Urey HC. Improvements in Mass Spectrometers for the Measurement of Small Differences in Isotope Abundance Ratios. *Review of Scientific Instruments*. 1950;21(8):724-730. doi:10.1063/1.1745698
65. Miller MF. Isotopic fractionation and the quantification of 17O anomalies in the oxygen three-isotope system: an appraisal and geochemical significance. *Geochim Cosmochim Acta*. 2002;66(11):1881-1889. doi:https://doi.org/10.1016/S0016-7037(02)00832-3
66. Meijer HAJ, Li WJ. The Use of Electrolysis for Accurate δ17O and δ18O Isotope Measurements in Water. *Isotopes Environ Health Stud*. 1998;34(4):349-369. doi:10.1080/10256019808234072
67. Passey BH, Hu H, Ji H, et al. Triple oxygen isotopes in biogenic and sedimentary carbonates. *Geochim Cosmochim Acta*. 2014;141:1-25. doi:https://doi.org/10.1016/j.gca.2014.06.006
68. Barkan E, Affek HP, Luz B, Bergel SJ, Voarintsoa NRG, Musan I. Calibration of δ17O and 17Oexcess values of three international standards: IAEA-603, NBS19 and NBS18. *Rapid Communications in Mass Spectrometry*. 2019;33(7):737-740. doi:https://doi.org/10.1002/rcm.8391

69. Wostbrock JAG, Cano EJ, Sharp ZD. An internally consistent triple oxygen isotope calibration of standards for silicates, carbonates and air relative to VSMOW2 and SLAP2. *Chem Geol*. 2020;533:119432. doi:https://doi.org/10.1016/j.chemgeo.2019.119432
70. Chipera SJ, Bish DL. Baseline Studies of the Clay Minerals Society Source Clays: Powder X-Ray Diffraction Analyses. *Clays Clay Miner*. 2001;49(5):398-409. doi:DOI: 10.1346/CCMN.2001.0490507
71. Pruett RJ, Webb HL. Sampling and Analysis of KGa-1B Well-Crystallized Kaolin Source Clay. *Clays Clay Miner*. 1993;41(4):514-519. doi:DOI: 10.1346/CCMN.1993.0410411
72. Mermut AR, Cano AF. Baseline Studies of the Clay Minerals Society Source Clays: Chemical Analyses of Major Elements. *Clays Clay Miner*. 2001;49(5):381-386. doi:DOI: 10.1346/CCMN.2001.0490504
73. Sakharov BA, Drits VA, McCarty DK, Walker GM. Modeling Powder X-ray Diffraction Patterns of the Clay Minerals Society Kaolinite Standards: KGa-1, KGa-1b, and KGa-2. *Clays Clay Miner*. 2016;64(3):314-333. doi:DOI: 10.1346/CCMN.2016.0640307
74. Morad S, Worden RH, Ketzer JM. Oxygen and Hydrogen Isotopic Composition of Diagenetic Clay Minerals in Sandstones: A Review of the Data and Controls. In: *Clay Mineral Cements in Sandstones*. ; 1999:63-91. doi:https://doi.org/10.1002/9781444304336.ch3
75. Munroe JS, Ryan PC, Proctor A. Pedogenic clay formation from allochthonous parent materials in a periglacial alpine critical zone. *Catena (Amst)*. 2021;203:105324. doi:https://doi.org/10.1016/j.catena.2021.105324
76. Menicucci AJ, Matthews JA, Spero HJ. Oxygen isotope analyses of biogenic opal and quartz using a novel microfluorination technique. *Rapid Communications in Mass Spectrometry*. 2013;27(16):1873-1881. doi:https://doi.org/10.1002/rcm.6642
77. Piccione G, Blackburn T, Tulaczyk S, et al. Subglacial precipitates record Antarctic ice sheet response to late Pleistocene millennial climate cycles. *Nat Commun*. 2022;13(1):5428. doi:10.1038/s41467-022-33009-1
78. Ibarra DE, Dai J, Gao Y, et al. High-elevation Tibetan Plateau before India–Eurasia collision recorded by triple oxygen isotopes. *Nat Geosci*. 2023;16(9):810-815.
79. Yeung LY, Young ED, Schauble EA. Measurements of 18O18O and 17O18O in the atmosphere and the role of isotope-exchange reactions. *Journal of Geophysical Research: Atmospheres*. 2012;117(D18). doi:https://doi.org/10.1029/2012JD017992
80. Swann GEA, Leng MJ, Juschus O, Melles M, Brigham-Grette J, Sloane HJ. A combined oxygen and silicon diatom isotope record of Late Quaternary change in Lake El'gygytgyn, North East Siberia. *Quat Sci Rev*. 2010;29(5):774-786. doi:https://doi.org/10.1016/j.quascirev.2009.11.024
81. Shemesh A, Yam R, Assulin M, Elish E. The triple oxygen isotope signature of uranium oxides in the nuclear fuel cycle. *Journal of Nuclear Materials*. 2024;590:154889.